Organic & Biomolecular Chemistry

ROYAL SOCIETY OF CHEMISTRY

PAPER

View Article Online
View Journal

Cite this: DOI: 10.1039/d0ob00122h

Construction of pH sensitive smart glutathione peroxidase (GPx) mimics based on pH responsive pseudorotaxanes†

Jiaxi Li, Wenlong Jia, Ganghui Ma, Xiaoyin Zhang, Shaojie An, Tao Wang and Shan Shi *

Received 19th January 2020,
Accepted 30th March 2020

DOI: 10.1039/d0ob00122h

rsc.li/obc

Two organoselenium compounds, both of which were modified with two primary amine groups, were designed and synthesized to mimic the catalytic properties of glutathione peroxidase (GPx). It was demonstrated that the catalytic mechanism of the diselenide organoselenium compound (compound **1**) was a ping-pong mechanism while that of the selenide organoselenium compound (compound **2**) was a sequential mechanism. The pH-controlled switching of the catalytic activities was achieved by controlling the formation and dissociation of the pseudorotaxanes based on the organoselenium compounds and cucurbit[6]uril (CB[6]). Moreover, the switching was reversible at pH between 7 and 9 for compound **1** or between 7 and 10 for compound **2**.

Introduction

Enzymes play an irreplaceable role *in vivo* because of their high rate and good stereoselectivity in catalysing biochemical reactions. In order to further explore their catalytic mechanism and extend their *in vitro* applications, much efforts have been devoted to the construction of various artificial enzymes over the past 50 years.[1–5] In the design of artificial enzymes, glutathione peroxidase (GPx), an antioxidant selenoenzyme, has attracted much attention.[6–9] GPx catalyses the reduction of hydroperoxides (ROOH) at the expense of tripeptide glutathione (GSH) and maintains the metabolic balance of reactive oxygen species (ROS) *in vivo* to protect various organisms from oxidative stress and to reduce the risk of a range of related diseases.[10–12]

Pioneering works on GPx mimics were carried out by Sies *et al.* who designed ebselen (2-phenyl-1,2-benzoisoselenazol-3(2*H*)-one) as a potential antioxidant medicine.[13,14] Encouraged by the successful design of ebselen, a series of organoselenium/tellurium compounds based on selenium/tellurium ether bonds have been reported.[15–19] Afterwards, in an attempt to simulate the cavity function of natural GPx, numerous host molecules, including cyclodextrin derivatives and antibodies modified by a selenium or tellurium catalytic centre, were studied.[20–24] Compared with organoselenium/tellurium compounds, these chemically operated host molecules possessed hydrophobic or hydrophilic cavities which could recognize different substrates. In this way, the concept of synergy of recognition and catalysis was proposed to obtain GPx mimics with higher efficiency. Similarly, molecularly imprinted GPx mimics were developed in view of transition state recognition by imitating the active site microenvironment of natural GPx.[25,26] In the recent two decades, with the booming development of supramolecular and nanoscientific strategies, various nanoenzyme models of GPx, including micelles, vesicles and nanotubes, have been demonstrated based on supramolecular nano-assemblies.[27–29] Moreover, the molecular imprinting strategy can also be used to mimic specific substrate binding sites of natural GPx at the surface of nanoenzyme models. The catalytic efficiency thus has had a significant enhancement. Furthermore, in order to obtain mimics that have a more similar catalytic structure to natural GPx, the genetic engineering strategy was exploited to construct a series of artificial seleno-proteins or telluro-proteins.[30–32]

Up to now, some of these GPx mimics have shown satisfactory enzymatic properties. Genetic engineering models even displayed extraordinarily high activities that rival the native ones.[32] On the other hand, the design and preparation of smart GPx mimics with controlled catalytic activity have also attracted increasing attention. The smart GPx mimics can be constructed using materials that are responsive to external stimuli such as temperature, light and pH. Several pioneering works have been reported by Liu and co-workers.[33–38] For

College of Materials Science and Engineering, Shenyang University of Chemical Technology, Shenyang 110142, People's Republic of China.
E-mail: sshi@syuct.edu.cn

†Electronic supplementary information (ESI) available: Characterization of compounds **1** and **2**, and catalytic curves of compounds **1** and **2** in enzymatic kinetics tests. See DOI: 10.1039/d0ob00122h

example, a photoresponsive GPx mimic was successfully designed by the supramolecular strategy using photocontrolled inclusion–exclusion reaction of azobenzene with telluride β-cyclodextrin (β-CD) dimers.[33] Moreover, GPx active sites were introduced into temperature responsive poly(*N*-isopropylacrylamide) scaffolds through the formation of microgels, micelles and nanotubes.[34–38] As expected, these temperature sensitive GPx mimics exhibited excellent GPx-like catalytic activity with typical saturation kinetics behaviours.

In the design of smart artificial enzymes, molecular machines which can be regulated by an external stimulus in different chemical processes are ideal scaffolds due to their dynamic properties and particular topological structures.[39–41] The development of pH responsive molecular machines provides an opportunity to construct pH sensitive GPx mimics. Such smart GPx mimics are promising in the future as potential medicines because the pH level in the human body varies in different cells and organs.[42] One of the classical pH responsive molecular machines is a pseudorotaxane based on cucurbit[6]uril (CB[6]). As a member of the cucurbit[n]uril (CB[*n*] *n* = 5–8) family, CB[6] is a macrocyclic compound with 6-glycoluril units and has a hydrophobic cavity that is accessible through two identical carbonyl-fringed portals.[43–49] CB[6] and di-protonated diaminoalkane can form a very stable 1 : 1 host–guest complex with a binding constant as high as 10^5–10^6 M^{-1}. However, the binding constant decreases significantly when the two nitrogen atoms are deprotonated.[50]

Inspired by the above works, we developed a pH sensitive GPx model by using a pseudorotaxane molecular switch formed by CB[6] and an organoselenium compound. We designed organoselenium compounds **1** and **2** (Fig. 1a) as GPx models, which contain two primary amine groups and a diselenide catalytic center (compound **1**) or a selenide catalytic center (compound **2**). In the presence of CB[6], the GPx mimics form 1 : 1 host–guest pseudorotaxane complexes when the amine groups are di-protonated. In this case, the mimics cannot show GPx activity since the active sites are encapsulated into the hydrophobic cavity of CB[6] (Fig. 1b). As the primary amine groups are gradually deprotonated with the rise of pH, the binding ability of CB[6] with compounds **1** and **2** significantly decreases. As a result, the active sites are exposed to the solution, causing an increase of GPx activity. Thus, the catalytic activity of the GPx model can be switched on/off through changing the pH.

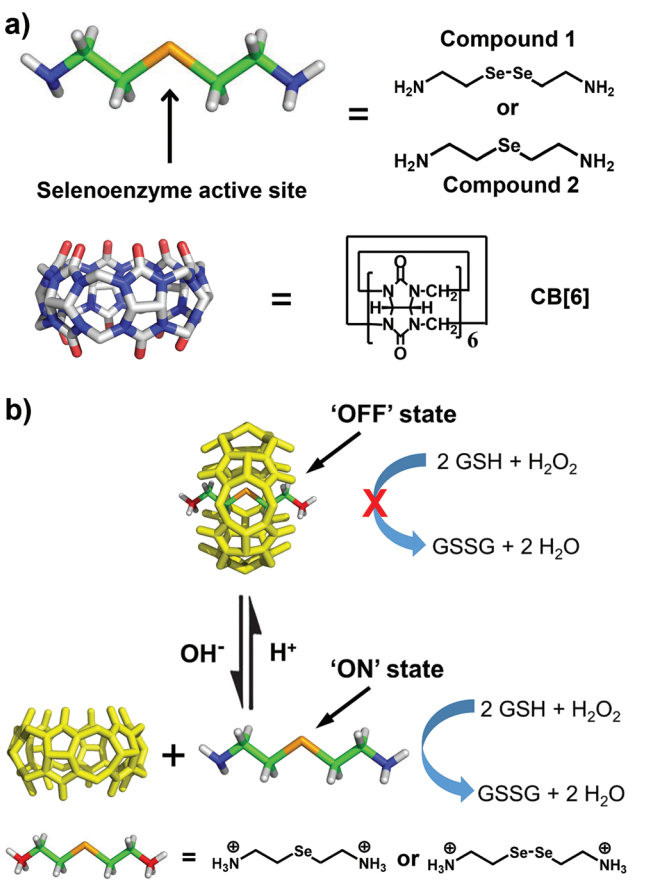

Fig. 1 (a) Structures of organoselenium compounds **1** and **2** and CB[6]; (b) schematic representation of the pH sensitive smart GPx mimic based on the formation and dissociation of pH responsive pseudorotaxanes formed by CB[6] and compounds **1** and **2**.

Results and discussion

Organoselenium compounds **1** and **2** were synthesized by the procedures shown in Fig. 2. After the synthesis, ^{1}H NMR titration experiments were performed at pH = 7 to test whether the synthesized compound **1** can form pseudorotaxane with CB[6]. As shown in Fig. 3a, upon the addition of CB[6] into compound **1** in D_2O, progressive disappearance of the signals corresponding to H_1 and H_2 of compound **1** occurred, followed by the growth of two new peaks. The appearance of the new peaks can be attributed to the movement of H_1 and H_2 of compound **1** due to its encapsulation inside CB[6]. After 1 equiv. of CB[6] was introduced, the original peaks corresponding to H_1 and H_2 disappeared completely. This indicates that CB[6] and compound **1** formed 1 : 1 host–guest pseudorotaxane complexes when the primary amine groups were protonated. It should be noted that, due to the formation of pseudorotaxane complexes, H_1 and H_2 showed different degrees of movement in ^{1}H NMR spectra (H_1 from 3.11 ppm to 2.61 ppm and H_2 from 3.36 ppm to 3.16 ppm). After compound **1** was completely incorporated into CB[6], H_1 was close to the internal part of the cavity while H_2 was close to the portal of the cavity, hence leading to the chemical shift movement of H_1 being obviously larger than H_2. The binding constant between compound **1** and CB[6] was calculated to be $1.19 \pm 0.09 \times 10^4$ M^{-1} at pH = 7 (Fig. S15†).

^{1}H NMR titration experiments were also utilized to confirm the formation of the pseudorotaxane based on CB[6] and compound **2**. The result was similar to that of compound **1** (Fig. 3b). After 1 equiv. of CB[6] was added, the H_1 and H_2 peaks due to compound **2** completely moved from 2.75 to 1.81 ppm and from 3.16 to 2.95 ppm, respectively. The binding

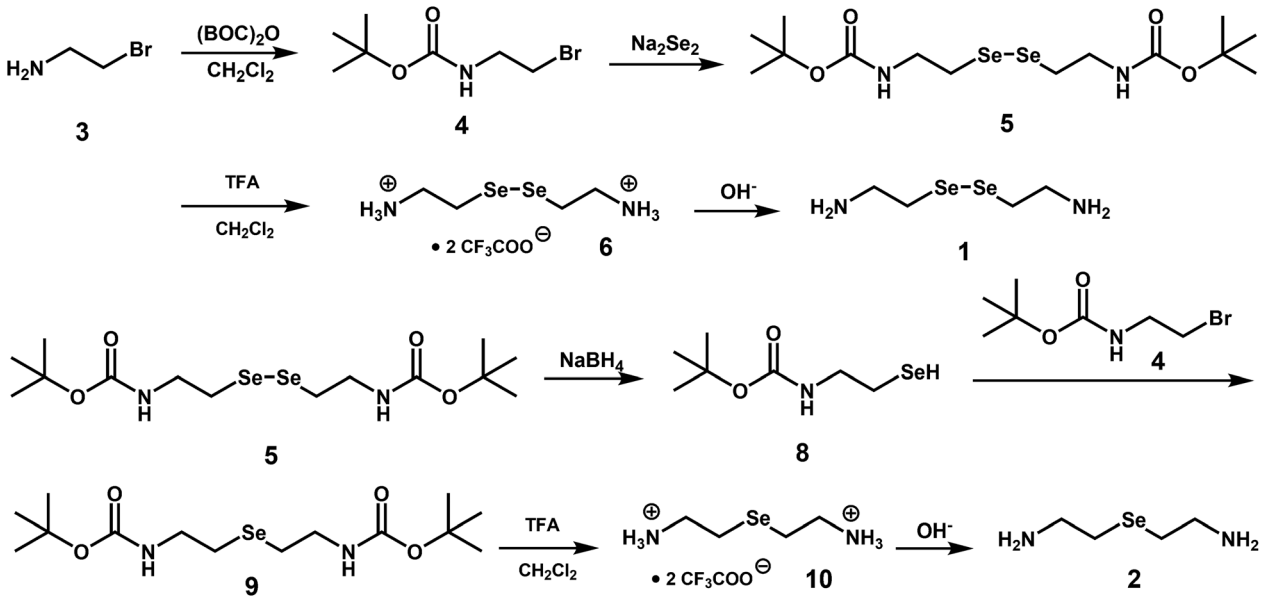

Fig. 2 Synthesis procedures of organoselenium compounds **1** and **2**.

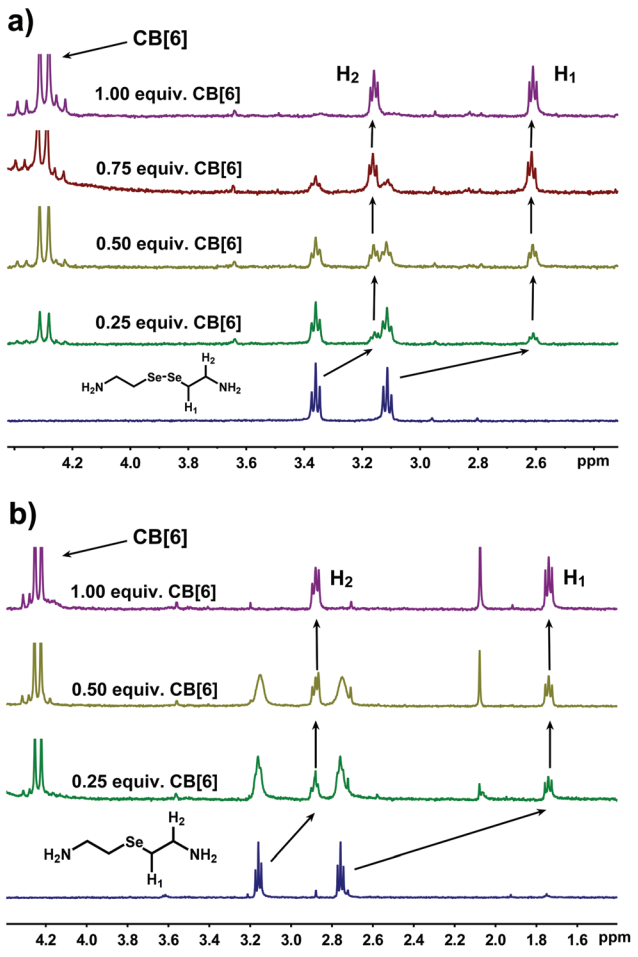

Fig. 3 (a) Partial ^{1}H NMR spectra (500 MHz) of compound **1** and mixtures of compound **1** (1 mmol L^{-1}) with different amounts of CB[6] at pH = 7. (b) Partial ^{1}H NMR spectra (500 MHz) of compound **2** and mixtures of compound **2** (1 mmol L^{-1}) with different amounts of CB[6] at pH = 7.

constant between compound **2** and CB[6] was calculated to be $2.50 \pm 0.10 \times 10^4$ M^{-1} at pH = 7 (Fig. S16†), about twice that of compound **1** with CB[6]. On the other hand, the binding constant between diaminopentane and CB[6] can be as high as 2.40×10^6 M^{-1} as reported in the literature.[50] After the middle carbon atom of the diaminopentane was replaced by a sulfur atom to form $H_2N(CH_2)_2S(CH_2)_2NH_2$, the binding constant was found to reduce by an order of magnitude to 4.2×10^5 M^{-1}. In the present study, we synthesized compound **2** by substituting a selenium atom, a same main group element as sulfur, for the sulfur atom of $H_2N(CH_2)_2S(CH_2)_2NH_2$. This resulted in the decline of the binding constant further to $2.50 \pm 0.10 \times 10^4$ M^{-1}. This is possibly because the size of methylene in diaminopentane matched the cavity of CB[6] best. As the middle carbon atom was replaced by sulfur and selenium atoms, the middle methylene changed to thioether and selenide, which increased the molecular size and thus decreased the binding constant with CB[6]. Moreover, when the selenide in compound **2** was replaced by the diselenide in compound **1**, the molecular size was further increased. As a result, the binding constant of compound **1** and CB[6] further decreased to $1.19 \pm 0.09 \times 10^4$ M^{-1}.

With the increase of pH, the binding ability of CB[6] with compound **1** or **2** significantly decreased followed by the dissociation of the pseudorotaxane. These were also studied by ^{1}H NMR (Fig. 4). Compound **1** formed the pseudorotaxane with 1 equiv. of CB[6] at pH = 7 as mentioned above. With the rise of pH, the amine groups of compound **1** were deprotonated, causing the dissociation of the pseudorotaxane. As a result, in ^{1}H NMR spectra, the peaks attributed to the encapsulated compound **1** showed a significant reduction followed by the increase of the peaks of free compound **1** (Fig. 4a). It is worth mentioning that the peaks of free compound **1** exhibited

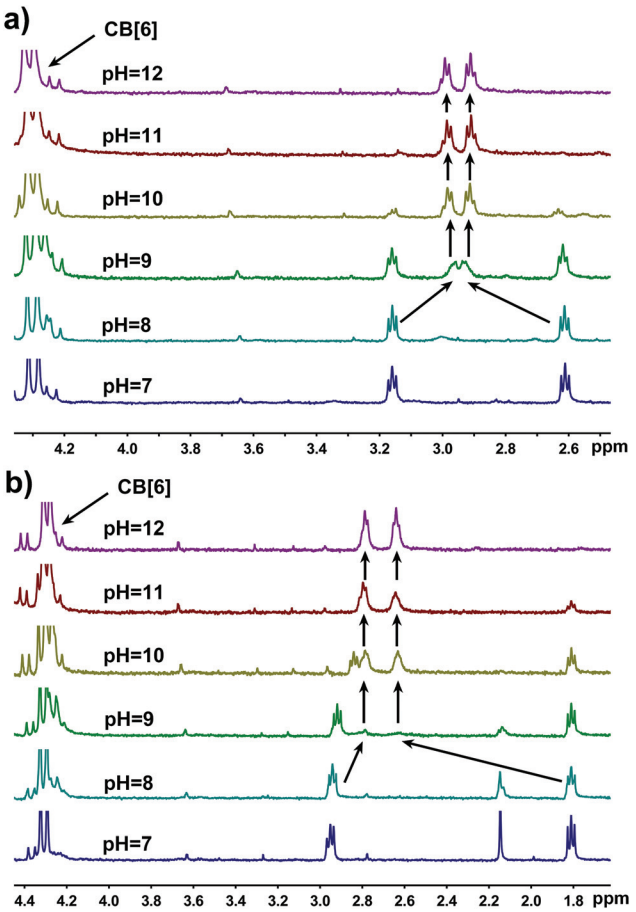

Fig. 4 Partial ^{1}H NMR spectra (500 MHz) of mixtures of (a) compound **1** (1 mmol L^{-1}) and (b) compound **2** (1 mmol L^{-1}) with CB[6] (1 mmol L^{-1}) at different pH values.

different chemical shifts at different pH values. At pH = 7, the two primary amine groups of compound **1** were protonated. In this case, the chemical shifts of H_1 and H_2 were 3.11 and 3.36 ppm, respectively (Fig. 3a). However, as the two primary amine groups changed from the protonated to deprotonated state at pH = 12, the chemical shifts of H_1 and H_2 had an obvious upfield movement (H_1 to 2.92 ppm and H_2 to 2.99 ppm). H_2 exhibited a larger movement of the chemical shift as compared to H_1 because H_2 was nearer to the amine groups than H_1. Through comparing the integral of peaks for the encapsulated and free compound **1**, we found from calculations that 17% of the pseudorotaxane was dissociated when the pH rose to 9. Moreover, the ratio of the dissociated pseudorotaxane increased to 72% when the pH rose to 10. At pH = 12, the pseudorotaxane formed almost totally dissociated with the ratio of the remaining pseudorotaxane less than 5%.

A similar result was observed for compound **2**. Compound **2** also formed a pseudorotaxane with 1 equiv. of CB[6] at pH = 7. The dissociation ratios of the pseudorotaxane were 15% and 57%, respectively, when the pH rose to 9 and 10. When the pH went up to 12, the ratio of the remaining pseudorotaxane was also less than 5% (Fig. 4b). It is obvious that, at the same pH, compound **1** exhibited a relatively high dissociation ratio of the pseudorotaxane as compared with compound **2**. This can be attributed to the lower binding constant between CB[6] and compound **1** as described above. The results indicate that the formation and dissociation of the pseudorotaxane based on CB[6] and compound **1** or **2** could be controlled by pH. That is, when CB[6] and compound **1** or **2** formed the pseudorotaxane at pH = 7, the active sites of compound **1** or **2** were encapsulated into the hydrophobic cavity of CB[6] and were unable to show their catalytic activities. In contrast, as part of the pseudorotaxane was dissociated at higher pH, the active sites of the free compound **1** or **2** were exposed to the solution and were capable of catalysing the corresponding reactions. Thus the GPx activity of compound **1** or **2** can be switched on/off by controlling the pH of the solution.

The catalytic activities of compounds **1** and **2** were first investigated in a 3-carboxy-4-nitrobenzenethiol (TNB) assay system at 37 °C and pH = 7. Catalytic curves for different concentrations of compounds **1** and **2** were obtained. As shown in Fig. 5, the slope of the catalytic curves displayed a linear increase with the increase of the concentration of compounds **1** and **2**, which was in accord with the typical enzymatic reaction. The GPx activities of compounds **1** and **2** were calculated to be $0.95 \pm 0.01 \times 10^{-3}$ and $2.69 \pm 0.04 \times 10^{-3}$ μmol min^{-1} μmol^{-1}, respectively. As compared to diphenyl diselenide

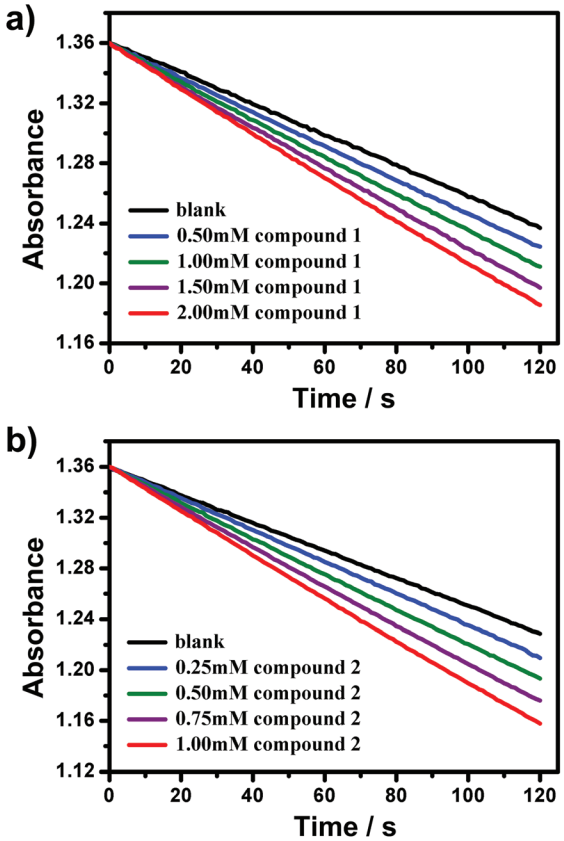

Fig. 5 Catalytic curves for different concentrations of (a) compound **1** and (b) compound **2** using the TNB assay system at pH = 7.

(PhSeSePh), a typical GPx mimic, the efficiency of compounds **1** and **2** increased by about an order of magnitude. Different from diphenyl diselenide, both compounds **1** and **2** have two amine groups. The amine groups can recognize the substrate (TNB) by the electrostatic interactions with the carboxyl groups of TNB, leading to the improvement of the catalytic activity. The GPx activities of compounds **1** and **2** at different pH values in the TNB assay system were also investigated. The GPx activities of compound **1** were 0.57 ± 0.06 × 10^{-3}, 0.95 ± 0.01 × 10^{-3}, 0.85 ± 0.03 × 10^{-3} and 0.70 ± 0.02 × 10^{-3} μmol min^{-1} $μmol^{-1}$ at pH = 6, 7, 8 and 9, respectively (Fig. 6a). The result indicates that the most suitable pH for compound **1** was 7. The GPx activities of compound **2** were 2.37 ± 0.14 × 10^{-3}, 2.69 ± 0.04 × 10^{-3}, 3.66 ± 0.07 × 10^{-3}, 4.31 ± 0.21 × 10^{-3} and 2.75 ± 0.16 × 10^{-3} μmol min^{-1} $μmol^{-1}$ at pH = 6, 7, 8, 9 and 10, respectively (Fig. 6b). Compound **2** showed its highest GPx activity at pH = 9. The GPx activity of compound **1** could not be measured at pH = 10 since the slope of the catalytic curves at 1 mM was even smaller than that of the blank.

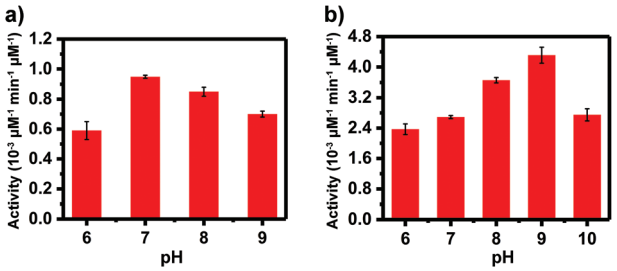

Fig. 6 Catalytic activities of (a) compound **1** and (b) compound **2** at different pH values using the TNB assay system.

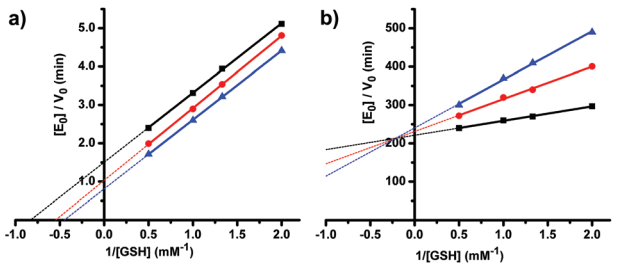

Fig. 7 Double-reciprocal plots of the reduction of H_2O_2 by GSH under the catalysis of (a) compound **1** and (b) compound **2**. [E_0] = total enzyme concentration; [E_0]/V_0 *versus* 1/[GSH] (mM^{-1}) at [H_2O_2] = 0.5 mM (▲), 0.75 mM (●) and 1.00 mM (■).

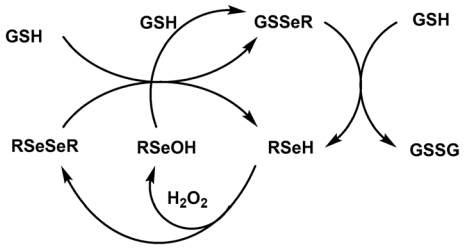

Fig. 8 Proposed catalytic mechanism of compound **1**.

To fully understand the difference in the behaviour of GPx activity between compounds **1** and **2**, we further investigated the enzyme kinetics with double-reciprocal plots using a GSH reductase-reduced nicotinamide adenine dinucleotide phosphate (NADPH) coupled assay. The assay involved the use of GSH and H_2O_2 as two substrates. The concentration of H_2O_2 was fixed and the GPx activities of compounds **1** or **2** were measured under different concentrations of GSH (Fig. S17–22†). The double-reciprocal plots were obtained from the GPx activity reciprocal *versus* GSH concentration reciprocal (Fig. 7). Similarly, the concentration of GSH was kept constant and the GPx activities of compound **1** or **2** were measured under different concentrations of H_2O_2 to obtain another double-reciprocal plot (Fig. S23 and S24†). The double-reciprocal plots of compound **1** yielded a series of parallel linear plots for both substrates (Fig. 7a and S23†), suggesting that the catalytic mechanism of compound **1** was a ping-pong mechanism with at least one covalent intermediate.[53–58] According to the detailed kinetic studies carried out by Engman[56] and Mugesh,[57] the catalytic intermediate of diselenide organoselenium compounds was a catalyst–substrate complex (RSeSR'). Herein, the catalytic reaction of compound **1** might proceed *via* the mechanism shown in Fig. 8. Saturation kinetics were observed for each of the enzymatic peroxidase reactions at all the individual concentrations of GSH and H_2O_2 investigated.

Table 1 Apparent kinetic parameters for H_2O_2 reduction by GSH catalyzed by compounds **1** and **2**

	Compound **1**			Compound **2**		
[H_2O_2] (mM)	k_{cat} (min^{-1})	K_{GSH} (M)	k_{cat}/K_{GSH} (M^{-1} min^{-1})	k_{cat} (min^{-1})	K_{GSH} (M)	k_{cat}/K_{GSH} (M^{-1} min^{-1})
0.5	0.66 ± 0.01	1.19 ± 0.01 × 10^{-3}	5.52 ± 0.07 × 10^2	4.16 ± 0.09 × 10^{-3}	5.24 ± 0.05 × 10^{-4}	7.94 ± 0.24
0.75	0.97 ± 0.02	1.82 ± 0.02 × 10^{-3}	5.32 ± 0.05 × 10^2	4.33 ± 0.09 × 10^{-3}	3.66 ± 0.09 × 10^{-4}	11.83 ± 0.53
1	1.23 ± 0.02	2.21 ± 0.03 × 10^{-3}	5.55 ± 0.03 × 10^2	4.52 ± 0.03 × 10^{-3}	1.70 ± 0.04 × 10^{-4}	26.55 ± 0.81
	Compound **1**			Compound **2**		
[GSH] (mM)	k_{cat} (min^{-1})	$K_{H_2O_2}$ (M)	$k_{cat}/K_{H_2O_2}$ (M^{-1} min^{-1})	k_{cat} (min^{-1})	$K_{H_2O_2}$ (M)	$k_{cat}/K_{H_2O_2}$ (M^{-1} min^{-1})
0.5	0.26 ± 0.01	1.72 ± 0.17 × 10^{-4}	1.51 ± 0.19 × 10^3	7.68 ± 3.97 × 10^{-3}	1.41 ± 0.51 × 10^{-3}	5.43 ± 1.32
1	0.52 ± 0.03	3.64 ± 0.16 × 10^{-4}	1.43 ± 0.14 × 10^3	6.05 ± 1.45 × 10^{-3}	6.34 ± 0.10 × 10^{-4}	9.54 ± 2.40
2	0.94 ± 0.07	6.35 ± 0.05 × 10^{-4}	1.48 ± 0.12 × 10^3	5.32 ± 0.58 × 10^{-3}	3.05 ± 0.51 × 10^{-4}	17.44 ± 4.13

The relevant steady-state equation for the enzymatic peroxidase reaction is as follows.

$$\frac{v_0}{[E_0]} = \frac{k_{cat}[GSH][H_2O_2]}{K_{mGSH}[H_2O_2] + K_{mH_2O_2}[GSH] + [GSH][H_2O_2]}$$

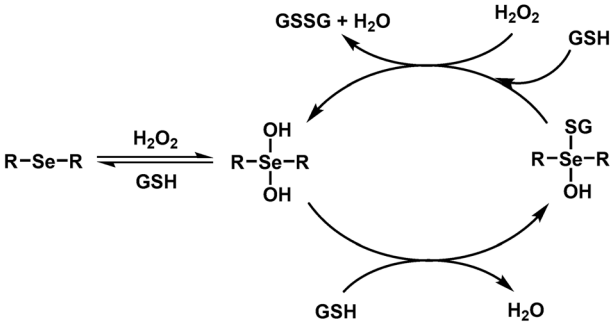

Fig. 9 Proposed catalytic mechanism of compound 2.

Here, v_0 is the initial reaction rate, $[E_0]$ is the initial enzyme mimic concentration, k_{cat} is a pseudo-first-order rate constant and $K_{mH_2O_2}$ and K_{mGSH} are the Michaelis–Menten constants for hydrogen peroxide and glutathione, respectively. The kinetic parameters of the enzymatic reactions of compound **1** were calculated according to the steady-state equation and double-reciprocal plots and are shown in Table 1.

In contrast to the double-reciprocal plots of compound **1**, those of compound **2** yielded a series of intersecting linear plots for both substrates (Fig. 7b and S24†), which indicates that the catalytic mechanism of compound **2** was a sequential mechanism. According to the studies by Carsol *et al.*[59] the single product (GSSG) was necessarily released in the last step in the sequential mechanism. Before the release of the product, both of the substrates formed an enzyme–substrate complex with the enzyme. Engman *et al.* and others systematically analysed the catalytic process of selenide organoselenium compounds and conjectured that the selenide organoselenium compounds were in their oxidized state ($RSe(OH)_2R$) in the catalytic cycle.[60–62] Combining the studies carried out by

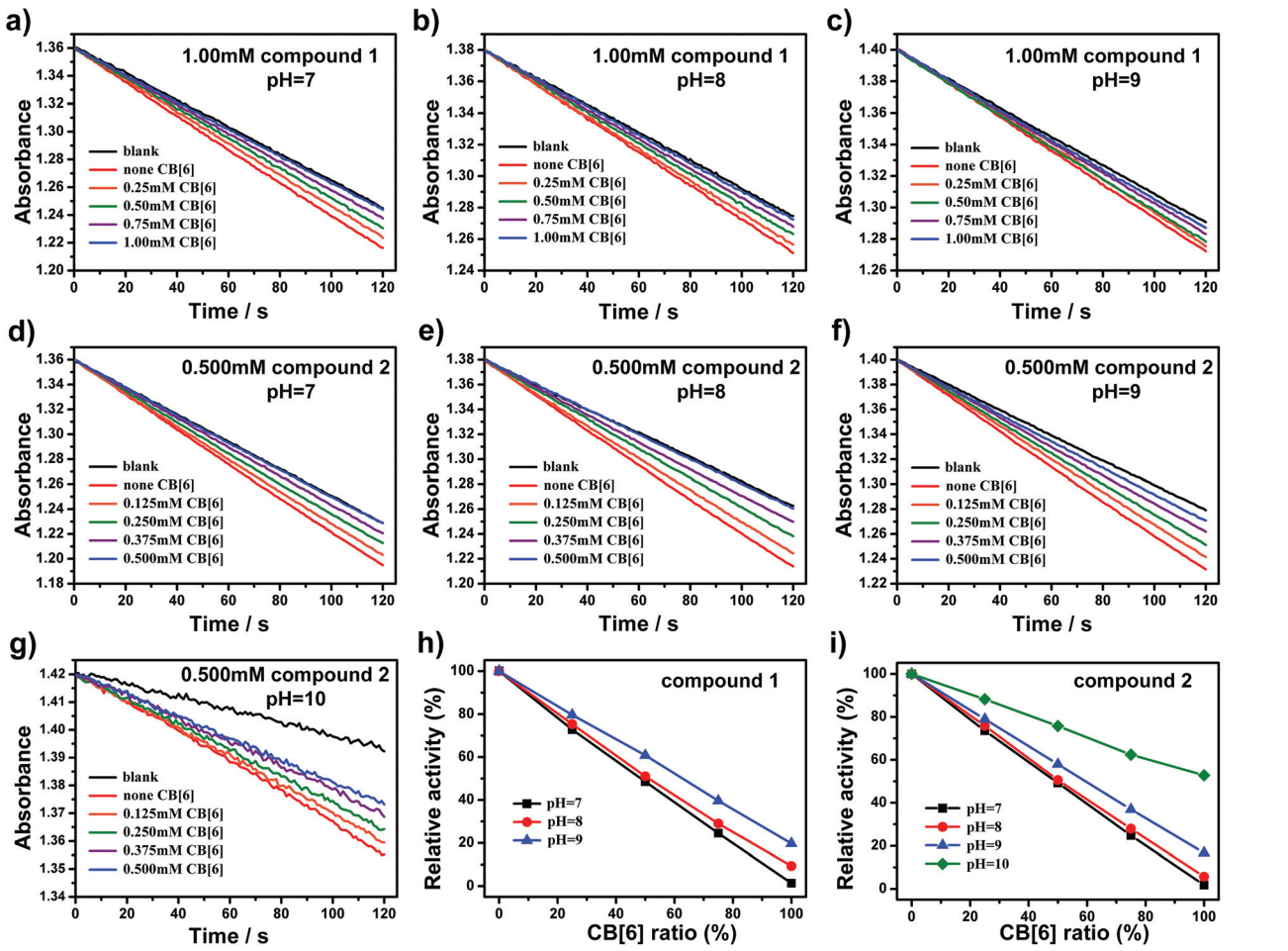

Fig. 10 Catalytic curves of compound **1** (1 mmol L^{-1}) and mixtures of compound **1** (1 mmol L^{-1}) with different amounts of CB[6] at (a) pH = 7, (b) pH = 8 and (c) pH = 9; catalytic curves of compound **2** (0.5 mmol L^{-1}) and mixtures of compound **2** (0.5 mmol L^{-1}) with different amounts of CB[6] at (d) pH = 7, (e) pH = 8, (f) pH = 9 and (g) pH = 10; decrease of relative activity *versus* mixtures of (h) compound **1** and (i) compound **2** with different amounts of CB[6] at different pH values. The activity of compound **1** or compound **2** without any CB[6] was defined as 100%.

Carsol and Engman, the catalytic reaction of compound **2** might proceed *via* the mechanism shown in Fig. 9. The relevant steady-state equation for compound **2** is identical to that for compound **1**. The kinetic parameters of the enzymatic reactions of compound **2** were calculated according to the steady-state equation and double-reciprocal plots and are also shown in Table 1.

The GPx activities of compounds **1** and **2**, after the formation of the pseudorotaxane with CB[6], were then evaluated using the TNB assay system. At pH = 7, compound **1** was diprotonated and had strong host–guest interactions with CB[6] to form the pseudorotaxane. Upon the addition of CB[6], the active sites of compound **1** were progressively enclosed by the hydrophobic cavity of CB[6], which led to a progressive decrease of GPx activity (Fig. 10a and h). After 1 equiv. CB[6] was added, the active sites of compound **1** were fully incorporated into CB[6] and could not come in contact with any substrate. As a result, compound **1** showed a very small activity of $1.40 \pm 0.83 \times 10^{-5}$ μmol min^{-1} $μmol^{-1}$ (Fig. 11a and b). A similar result was found upon the addition of CB[6] to compound **2** at pH = 7 (Fig. 11d and i). After the addition of 1 equiv. CB[6], compound **2** also hardly showed any activity ($4.68 \pm 1.86 \times 10^{-5}$ μmol min^{-1} $μmol^{-1}$, Fig. 11c and d). These results indicate that the formation of the pseudorotaxane between CB[6] and compound **1** or **2** could switch off the GPx activity, irrespective of the catalytic mechanism of compound **1** or **2**. However, when the solution was adjusted to a pH above 7, the pseudorotaxane started to partly dissociate because of the deprotonation of amine groups. At pH = 9, a decrease of the GPx activity of compound **1** occurred upon the addition of CB[6] (Fig. 10c and h). However, after 1 equiv. CB[6] was added, there was still about 20% activity ($0.14 \pm 0.01 \times 10^{-3}$ μmol min^{-1} $μmol^{-1}$) relative to compound **1** without CB[6] (Fig. 11a and b). As a result, the GPx activity of the pseudorotaxane formed by CB[6] and compound **1** can be switched on/off through changing the pH between 7 and 9. A similar result was also found when adding CB[6] to compound **2** at pH = 9 (Fig. 10f and i). After 1 equiv. CB[6] was added, there was still about 15% activity ($0.59 \pm 0.07 \times 10^{-3}$ μmol min^{-1} $μmol^{-1}$) as compared to that of compound **2** without CB[6] (Fig. 11c and d). Moreover, when the pH was increased to 10, the GPx activity of compound **2** remained more that 50% after 1 equiv. CB[6] was added ($1.45 \pm 0.02 \times 10^{-3}$ μmol min^{-1} $μmol^{-1}$, Fig. 10g, 11c and d). As a result, the GPx activity of the pseudorotaxane formed by CB[6] and compound **2** could be switched on/off to a greater extent through changing the pH between 7 and 10.

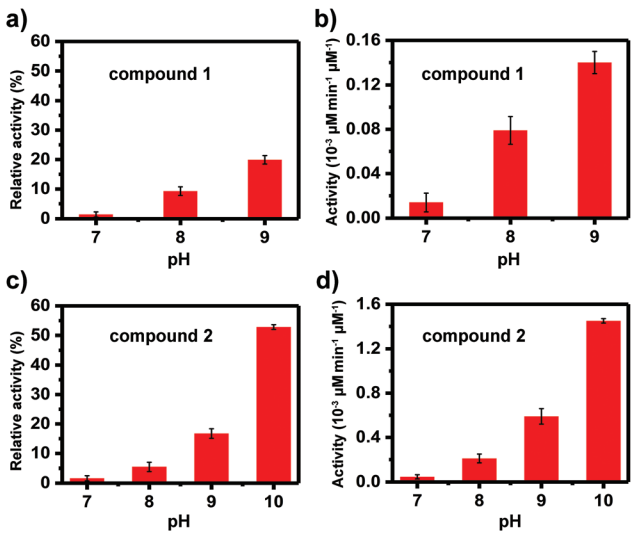

Fig. 11 (a) Relative catalytic activities and (b) catalytic activities of the pseudorotaxane formed by CB[6] and compound **1** at a range of pH from 7 to 9; (c) relative catalytic activities and (d) catalytic activities of the pseudorotaxane formed by CB[6] and compound **2** at a range of pH from 7 to 10.

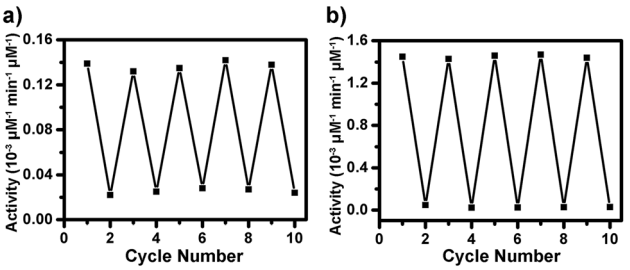

Fig. 12 (a) The ON–OFF switch of the catalytic activity of the pseudorotaxane formed by CB[6] and compound **1** by a change in pH between 7 and 9. (b) The ON–OFF switch of the catalytic activity of the pseudorotaxane formed by CB[6] and compound **2** by a change in pH between 7 and 10.

The above investigations demonstrate that the GPx activity of the pseudorotaxane formed by CB[6] and compound **1** or **2** can be switched on/off by changing the pH. As switchable GPx models, the reversibility of the catalytic activity of the pseudorotaxanes was also tested. The results reveal that the catalytic activities of two enzymes were completely reversible after multiple changes in pH between 7 and 9 for compound **1** (Fig. 12a) or between 7 and 10 for compound **2** (Fig. 12b).

Conclusions

In conclusion, we designed and synthesized two organoselenium compounds to mimic the catalytic properties of glutathione peroxidase (GPx). Organoselenium compound **1** contained a diselenide active centre while organoselenium compound **2** contained a selenide active centre. The catalytic mechanisms of the two organoselenium compounds were investigated in detail. The results indicate that compound **1** catalysed the reaction with a ping-pong mechanism while compound **2** with a sequential mechanism. Moreover, the GPx activity can be switched on and off by controlling the formation and dissociation of the pseudorotaxane based on CB[6] and the organoselenium compounds. Thus the reversible pH-controlled switching of catalytic activities was achieved even after multiple changes in pH between 7 and 9 (compound **1**)

or between 7 and 10 (compound **2**). We believe that the successful construction of such pH sensitive smart GPx mimics will provide a novel route to the design of smart artificial enzymes.

Experimental

Synthesis of compound 5

Selenium (1737.1 mg, 22.0 mmol) and sodium borohydride (756.6 mg, 20.0 mmol) were added into a 250 mL round bottom flask under the protection of nitrogen, followed by the injection of 20 mL deoxygenated water. After 30 min selenium reacted completely to give Na_2Se_2. Compound **4** (4.48 g, 20.0 mmol; see the ESI for its synthesis, Fig. S1†) was dissolved in 100 mL methyl alcohol and deoxygenated with nitrogen. The deoxygenated solution of compound **4** was injected into the round bottom flask and stirred for 12 hours at room temperature. The volatiles were removed under reduced pressure and the residue was transferred to a 500 mL separating funnel using 200 mL dichloromethane. The dichloromethane solution was extracted with sodium chloride solution (3 × 100 mL) and then the organic phase was dried with anhydrous sodium sulfate. The volatiles were removed and the residue was purified by column chromatography (silica gel, dichloromethane/ethyl acetate: 15/1 as eluent) to give a yellow solid **5** (4.0 g, 45% yield).

^{1}H NMR (500 MHz; $CDCl_3$; Me_4Si) δ 1.46 (18H, s, $2C(Me)_3$) 3.02 (4H, t, J = 7.0 Hz, $SeCH_2$) 3.48 (4H, t, J = 7.0 Hz, NCH_2) (Fig. S2†).

^{13}C NMR (500 MHz; $CDCl_3$; Me_4Si) δ 153.33, 76.95, 74.85, 74.60, 74.35, 38.40, 26.84, 25.90 (Fig. S3†).

High resolution ESI-TOF mass spectrum (m/z) calculated to be 448.0380 and found to be 449.0392 ($M + H^+$) and 471.0210 ($M + Na^+$) (Fig. S4†). The mass spectrum contained about thirteen isotopic peaks (from 441.0 to 453.0 and 463.0 to 475.0) which were typical isotopic peaks of the diselenide organoselenium compound.

Synthesis of compound 1

Compound **5** (4.0 g, 8.9 mmol) was added to a mixture of 10 mL dichloromethane and 10 mL trifluoroacetic acid in a 100 mL round bottom flask and stirred for 12 hours at room temperature. Most of the volatiles were removed under reduced pressure and the residue was deposited with 500 mL cold ethyl ether. A primrose yellow precipitate (compound **6**, 4.1 g, 96% yield) was obtained by filtration under reduced pressure and was dissolved in 50 mL saturated sodium carbonate solution. After extracting with ethyl acetate (3 × 30 mL), the organic phase was dried with anhydrous sodium sulfate. The volatiles were removed under reduced pressure to give a transparent primrose yellow liquid **1** (1.5 g, 68% yield).

^{1}H NMR (500 MHz; D_2O) δ 3.11 (4H, t, J = 7.0 Hz, $SeCH_2$) 3.37 (4H, t, J = 7.0 Hz, NCH_2) (Fig. S5†).

^{13}C NMR (500 MHz; D_2O) δ 39.60, 23.51 (Fig. S6†).

High resolution ESI-TOF mass spectrum (m/z) calculated to be 247.9931 and found to be 248.9427 ($M + H^+$) (Fig. S7†). The mass spectrum contained about thirteen isotopic peaks (from 240.9 to 252.9) which were typical isotopic peaks of the diselenide organoselenium compound.

Synthesis of compound 9

Compound **5** (3.0 g, 6.7 mmol) was dissolved to 50 mL methyl alcohol in a 100 mL round bottom flask and deoxygenated with nitrogen. Sodium borohydride (1.2 g, 31.7 mmol) was added into a 250 mL round bottom flask under the protection of nitrogen. 50 mL deoxygenated methyl alcohol solution of compound **5** was injected into the 250 mL round bottom flask. After 30 min the solution completely changed from yellow to colourless and transparent, indicating that compound **5** had totally reacted, giving compound **8**. Compound **4** (3.0 g, 13.5 mmol) was dissolved in 50 mL methyl alcohol and deoxygenated with nitrogen. The deoxygenated solution of compound **4** was injected into the methyl alcohol solution of compound **8** and stirred for 12 hours at room temperature. The volatiles were removed under reduced pressure and the residue was transferred to a 500 mL separating funnel using 200 mL dichloromethane. The dichloromethane solution was extracted with sodium chloride solution (3 × 100 mL) and then the organic phase was dried with anhydrous sodium sulfate. The volatiles were removed and the residue was purified by column chromatography (silica gel, dichloromethane/ethyl acetate: 15/1 as eluent) to give a transparent liquid **9** (3.7 g, 75% yield).

^{1}H NMR (500 MHz; $CDCl_3$; Me_4Si) δ 1.46 (18H, s, $2C(Me)_3$) 2.70 (4H, t, J = 7.0 Hz, $SeCH_2$) 3.37 (4H, t, J = 7.0 Hz, NCH_2) (Fig. S8†).

^{13}C NMR (500 MHz; $CDCl_3$; Me_4Si) δ 153.28, 76.82, 74.87, 74.61, 74.36, 37.97, 25.85, 21.54 (Fig. S9†).

High resolution ESI-TOF mass spectrum (m/z) calculated to be 368.1214 and found to be 369.1316 ($M + H^+$) and 391.1137 ($M + Na^+$) (Fig. S10†). The mass spectrum contained seven isotopic peaks (from 365.1 to 371.1 and 387.1 to 393.1) which were typical isotopic peaks of the selenide organoselenium compound.

Synthesis of compound 2

Compound **9** (3.7 g, 10.1 mmol) was added to a mixture of 10 mL dichloromethane and 10 mL trifluoroacetic acid in a 100 mL round bottom flask and stirred for 12 hours at room temperature. Most of the volatiles were removed under reduced pressure and the residue was deposited with 500 mL cold ethyl ether. The white precipitate (compound **10**, 3.7 g, 93% yield) was obtained by filtration under reduced pressure and dissolved in 50 mL saturated sodium carbonate solution. After extracting with ethyl acetate (3 × 30 mL), the organic phase was dried with anhydrous sodium sulfate. The volatiles were removed under reduced pressure to give a transparent liquid **2** (1.2 g, 71% yield).

^{1}H NMR (500 MHz; D_2O) δ 2.75 (4H, t, J = 7.0 Hz, $SeCH_2$) 3.16 (4H, t, J = 7.0 Hz, NCH_2) (Fig. S11†).

^{13}C NMR (500 MHz; D_2O) δ 38.98, 19.10 (Fig. S12†).

High resolution ESI-TOF mass spectrum (m/z) calculated to be 247.9931 and found to be 169.0218 ($M + H^+$) (Fig. S13†). The mass spectrum contained seven isotopic peaks (from 165.0 to 171.0) which were typical isotopic peaks of the selenide organoselenium compound.

^{1}H NMR titration experiment

Compound **1** was dissolved in D_2O at a concentration of 2.0 mmol L^{-1}. CB[6] was dissolved in 1 mol L^{-1} KCl aqueous (D_2O) solution at the concentrations of 0.5, 1.0, 1.5 and 2.0 mmol L^{-1}, respectively. The solutions of compound **1** and CB[6] were mixed at a ratio of 1 : 1 to give a mixture of compound **1** and 0.25, 0.50, 0.75 and 1.00 equiv. CB[6] in D_2O. In order to investigate the change of the interaction between CB[6] and compound **1** at different pH values, CF_3COOD and NaOD were utilized to control the pH of the mixture in a range of 7–12. ^{1}H NMR titration experiment of compound **2** was the same as that of compound **1**. All the experiments were performed in triplicate.

$$2\mathrm{TNB} + \mathrm{H_2O_2} \xrightarrow{\text{enzyme}} \mathrm{DTNB} + 2\mathrm{H_2O}$$

TNB catalytic activity assay system

A TNB (3-carboxy-4-nitrobenzenethiol) assay system, proposed by Hilvert *et al.*,[51] is an improved GPx catalytic activity assay method using TNB as a glutathione (GSH) alternative. The reaction equation has been shown above. The assay mixture contained 50 mM phosphate buffer (pH = 7–10), 100 μM TNB, 250 μM hydrogen peroxide (H_2O_2) and 250–1000 μM enzyme (compound **1** or **2**). The initial rate (v_0) for the reduction of H_2O_2 by TNB was determined by monitoring the UV absorption at 410 nm due to the thiolate (TNB). The definition of catalytic activity is the required enzyme quantity to oxidize 1 μM TNB per minute. The unit of catalytic activity is μM min^{-1} μM^{-1}. All the experiments were performed in triplicate.

$$2\mathrm{GSH} + \mathrm{H_2O_2} \xrightarrow{\text{enzyme}} \mathrm{GSSG} + 2\mathrm{H_2O}$$

$$\mathrm{GSSG} + \mathrm{NADPH} + \mathrm{H^+} \xrightarrow{\text{GSSG reductase}} 2\mathrm{GSH} + \mathrm{NADP^+}$$

GSH reductase-reduced NADPH coupled catalytic activity assay system

The GSH reductase-reduced nicotinamide adenine dinucleotide phosphate (NADPH) coupled assay system is a classical GPx catalytic activity assay method using GSH as the substrate, and is the same with natural GPx.[52] The reaction equation has been shown above. The assay mixture contained 50 mM phosphate buffer (pH = 7.0), 1 mM GSH, 500 μM hydrogen peroxide (H_2O_2), 1 U glutathione reductase (GR), 300 μM NADPH and 250–1000 μM enzyme (compound **1** or **2**). The initial rate (v_0) of the reduction of H_2O_2 by TNB was determined by monitoring the UV absorption at 340 nm due to the NADPH. The definition of catalytic activity is the required enzyme quantity to oxidize 1 μM NADPH per minute. The unit of catalytic activity is μM min^{-1} μM^{-1}. All the experiments were performed in triplicate.

Conflicts of interest

There are no conflicts to declare.

Acknowledgements

This work was supported by the Natural Science Foundation of China (no. 51573100), Educational Commission of Liaoning Province, China (no. LQ2019006) and Doctoral Scientific Research Foundation of Liaoning Science and Technology Department, China (no. 201601203).

Notes and references

1 A. J. Kirby, *Angew. Chem., Int. Ed. Engl.*, 1996, **35**, 707.
2 R. Breslow and S. Dong, *Chem. Rev.*, 1998, **98**, 1997.
3 G. Wulff, *Chem. Rev.*, 2002, **102**, 1.
4 M. Raynal, P. Ballester, A. Vidal-Ferran and P. W. N. M. van Leeuwen, *Chem. Soc. Rev.*, 2014, **43**, 1660.
5 M. Raynal, P. Ballester, A. Vidal-Ferran and P. W. N. M. van Leeuwen, *Chem. Soc. Rev.*, 2014, **43**, 1734.
6 G. Mugesh, W. W. du Mont and H. Sies, *Chem. Rev.*, 2001, **101**, 2125.
7 G. Mugesh and H. Singh, *Chem. Soc. Rev.*, 2000, **29**, 347.
8 X. Huang, X. M. Liu, Q. Luo, J. Q. Liu and J. C. Shen, *Chem. Soc. Rev.*, 2011, **40**, 1171.
9 Z. Y. Dong, Q. Luo and J. Q. Liu, *Chem. Soc. Rev.*, 2012, **41**, 7890.
10 J. T. Rotruck, A. L. Pope, H. E. Ganther, A. B. Swanson, D. G. Hafeman and W. G. Hoekstra, *Science*, 1973, **179**, 588.
11 L. Flohe, W. A. Gunzler and H. H. Schock, *FEBS Lett.*, 1973, **32**, 132.
12 L. Flohe, G. Loschen, W. A. Gunzler and E. Eichele, *Hoppe-Seyler's Z. Physiol. Chem.*, 1972, **352**, 987.
13 H. Sies, *Free Radical Biol. Med.*, 1993, **14**, 313.
14 H. Sies and H. Masumoto, *Adv. Pharmacol.*, 1997, **38**, 229.
15 T. G. Back and Z. Moussa, *J. Am. Chem. Soc.*, 2003, **125**, 13455.
16 Y. You, K. Ahsan and M. R. Detty, *J. Am. Chem. Soc.*, 2003, **125**, 4918.
17 S. S. Zade, H. B. Singh and R. J. Butcher, *Angew. Chem., Int. Ed.*, 2004, **43**, 4513.
18 S. Tomoda and M. Iwaoka, *J. Am. Chem. Soc.*, 1994, **116**, 2557.
19 M. McNaughton, L. Engman, A. Birmingham, G. Powis and I. A. Cotgreave, *J. Med. Chem.*, 2004, **47**, 233.
20 Z. Wu and D. Hilvert, *J. Am. Chem. Soc.*, 1990, **112**, 5647.
21 G. M. Luo, Z. Q. Zhu, L. Ding, G. Gao, Q. A. Sun, Z. Liu, T. S. Yang and J. C. Shen, *Biochem. Biophys. Res. Commun.*, 1994, **198**, 1240.

22 J. Q. Liu, S. J. Gao, G. M. Luo, G. L. Yan and J. C. Shen, *Biochem. Biophys. Res. Commun.*, 1998, **247**, 397.
23 G. M. Luo, X. J. Ren, J. Q. Liu, Y. Mu and J. C. Shen, *Curr. Med. Chem.*, 2003, **10**, 1151.
24 X. Huang, Y. Z. Yin and J. Q. Liu, *Macromol. Biosci.*, 2010, **10**, 1385.
25 X. Huang, Y. Liu, K. Liang, Y. Tang and J. Q. Liu, *Biomacromolecules*, 2008, **9**, 1467.
26 X. Huang, Y. Z. Yin, Y. Liu, X. L. Bai, Z. M. Zhang, J. Y. Xu, J. C. Shen and J. Q. Liu, *Biosens. Bioelectron.*, 2009, **25**, 657.
27 X. Zhang, H. P. Xu, Z. Y. Dong, Y. P. Wang, J. Q. Liu and J. C. Shen, *J. Am. Chem. Soc.*, 2004, **126**(34), 10556.
28 H. P. Xu, J. Gao, Y. P. Wang, Z. Q. Wang, M. Smet, W. Dehaenb and X. Zhang, *Chem. Commun.*, 2006, 796.
29 Y. Tang, L. P. Zhou, J. X. Li, Q. Luo, X. Huang, P. Wu, Y. G. Wang, J. Y. Xu, J. C. Shen and J. Q. Liu, *Angew. Chem., Int. Ed.*, 2010, **49**, 3920.
30 S. Boschi-Muller, S. Muller, A. V. Dorsselaer, A. Bock and G. Branlant, *FEBS Lett.*, 1998, **439**, 241.
31 S. Z. Mao, Z. Y. Dong, J. Q. Liu, X. Q. Li, X. M. Liu, G. M. Luo and J. C. Shen, *J. Am. Chem. Soc.*, 2005, **127**, 115883.
32 X. M. Liu, L. A. Silks, C. P. Liu, M. Ollivault-Shiflett, X. Huang, J. Li, G. M. Luo, Y. M. Hou, J. Q. Liu and J. C. Shen, *Angew. Chem., Int. Ed.*, 2009, **48**, 2020.
33 P. Wu, R. Q. Xiao, C. Q. Zhang, L. P. Zhou, Q. Luo, J. Y. Xu and J. Q. Liu, *Catal. Lett.*, 2010, **138**, 62.
34 X. Huang, Y. Z. Yin, X. Jiang, Y. Tang, J. Y. Xu, J. Q. Liu and J. C. Shen, *Macromol. Biosci.*, 2009, **9**, 1202.
35 X. Huang, Y. Z. Yin, Y. Tang, X. L. Bai, Z. M. Zhang, J. Y. Xu, J. Q. Liu and J. C. Shen, *Soft Matter*, 2009, **5**, 1905.
36 Y. Z. Yin, L. Wang, H. Y. Jin, C. Y. Lv, S. J. Yu, X. Huang, Q. Luo, J. Y. Xu and J. Q. Liu, *Soft Matter*, 2011, **7**, 2521.
37 L. Wang, H. X. Zou, Z. Y. Dong, L. P. Zhou, J. X. Li, Q. Luo, J. Y. Zhu, J. Y. Xu and J. Q. Liu, *Langmuir*, 2014, **30**, 4013.
38 H. X. Zou, H. C. Sun, L. Wang, L. L. Zhao, J. X. Li, Z. Y. Dong, Q. Luo, J. Y. Xu and J. Liu, *Soft Matter*, 2016, **12**, 1192.
39 E. R. Kay, D. A. Leigh and F. Zerbetto, *Angew. Chem., Int. Ed.*, 2007, **46**, 72.
40 M. Schmittel, S. De and S. Pramanik, *Angew. Chem., Int. Ed.*, 2012, **51**, 3832.
41 V. Blanco, A. Carlone, K. D. Hanni, D. A. Leigh and B. Lewandowski, *Angew. Chem., Int. Ed.*, 2012, **51**, 5166.
42 J. X. Li, C. Y. Si, H. C. Sun, J. Y. Zhu, T. Z. Pan, S. D. Liu, Z. Y. Dong, J. Y. Xu, Q. Luo and J. Q. Liu, *Chem. Commun.*, 2015, **51**, 9987.
43 K. Kim, *Chem. Soc. Rev.*, 2002, **31**, 96.
44 H. Cong, X. L. Ni, X. Xiao, Y. Huang, Q. J. Zhu, S. F. Xue, Z. L. F. Lindoy and G. Wei, *Org. Biomol. Chem.*, 2016, **14**, 4335.
45 L. Isaacs, *Acc. Chem. Res.*, 2014, **47**, 2052.
46 L. Liu, N. Nouvel and O. A. Scherman, *Chem. Commun.*, 2009, 3243.
47 S. Gürbüz, M. Idris and D. Tuncel, *Org. Biomol. Chem.*, 2015, **13**, 330.
48 Q. W. Zhang, X. Y. Yao, D. H. Qu and X. Ma, *Chem. Commun.*, 2014, **50**, 1567.
49 H. Cong, X. L. Ni, X. Xiao, Y. Huang, Q. J. Zhu, S. F. Xue, Z. Tao, L. F. Lindoy and G. Wei, *Org. Biomol. Chem.*, 2016, **14**, 4335.
50 J. Lagona, P. Mukhopadhyay, S. Chakrabarti and L. Isaacs, *Angew. Chem., Int. Ed.*, 2005, **44**, 4844.
51 I. M. Bell and D. Hilvert, *Biochemistry*, 1993, **32**, 13969.
52 H. J. Yu, J. Q. Liu, A. Bock, J. Li, G. M. Luo and J. C. Shen, *J. Biol. Chem.*, 2005, **280**, 11930.
53 K. Dalziel, *Biochem. J.*, 1969, **114**, 547.
54 L. Flohe, G. Loschen, W. A. Gunzler and E. Eichele, *Hoppe-Seyler's Z. Physiol. Chem.*, 1972, **353**, 987.
55 Z. Y. Dong, J. Q. Liu, S. Z. Mao, X. Huang, B. Yang, X. J. Ren, G. M. Luo and J. C. Shen, *J. Am. Chem. Soc.*, 2004, **126**, 16395.
56 L. Engman, D. Stern, I. A. Cotgreave and C. M. Andersson, *J. Am. Chem. Soc.*, 1992, **114**, 9737.
57 G. Mugesh, A. Panda, H. B. Singh, N. S. Punekar and R. J. Butcher, *J. Am. Chem. Soc.*, 2001, **123**, 839.
58 F. Ursini, M. Maiorini and C. Gregolin, *Biochim. Biophys. Acta*, 1982, **710**, 197.
59 M. A. Carsol, I. Pouliquen-Sonaglia, G. Lesgards, G. Marchis-Mouren, A. Puigserver and M. Santimone, *Eur. J. Biochem.*, 1997, **247**, 248.
60 S. R. Wilson, P. A. Zucker, R. R. C. Huang and A. Spector, *J. Am. Chem. Soc.*, 1989, **111**, 5936.
61 L. Engman, D. Stern, I. A. Cotgrware and C. M. Andersson, *J. Am. Chem. Soc.*, 1992, **114**, 9737.
62 M. Iwaoka and S. Tomoda, *J. Am. Chem. Soc.*, 1994, **116**, 2557.